Spectral response of wheat and lettuce to copper pollution

ZHU Yeqing[1,2], QU Yonghua[1,2], LIU Suhong[1,2], CHEN Shengbo[3]

1. *State Key Laboratory of Remote Sensing Science, Research Center for Remote Sensing and GIS, and School of Geography, Beijing Normal University. Beijing* 100875, *China*;
2. *Beijing Key Laboratory of Remote Sensing and Digital City Environment, Beijing* 100875, *China*;
3. *Earth Exploration Science and Technology Institute of Jilin University, Changchun* 130026, *China*

Abstract: The leaf reflectance spectra of plants polluted with heavy metal copper exhibit abnormal behavior. This paper investigates the spectral changes in copper-polluted leaves using seven spectral signatures and the spectral angle method. Wheat and lettuce were selected as the experimental subjects and were cultured in copper-polluted soil. Leaf spectra reflectance and scanning electron micrograph of ten copper treatment groups were measured in four regular periods. The reflectance spectra of the leaves were obtained using an ASD Field Spectrometer. Results showed that the irregular spectral changes of copper-polluted leaves depend on crop growth stages and crop types. The spectral angle, a simple method of comparing the vector angle of the leaf spectra with the given threshold values, has been justified as an efficient method of describing the spectral differences between copper-polluted leaves and healthy leaves. The method is very sensitive to light and the severity of copper pollution. Results also show that the leaf structural parameter (N) of copper-polluted leaves is larger than that of healthy leaves. The linear relationship between N and the reflectance value of the red shoulder was fitted with a correlation coefficient of 0.978. As a result, the deduced N from the leaf reflectance spectra may be used as an indicator to reflect the leaf structure distortion under copper pollution conditions. The significance of this study lies in its provision of data asbasis and theoretical support for the construction of a copper-polluted leaf reflectance spectral model.

Key words: heavy metal pollution, leaf reflectance spectra, characteristic wavelength, spectral angle, PROSPECT model

CLC number: X87 **Document code:** A

Citation format: Zhu Y Q, Qu Y H, Liu S H and Chen S B. 2014. Spectral response of wheat and lettuce to copper pollution. Journal of Remote Sensing, 18(2): 335-352 [DOI: 10.11834/jrs.20143073]

1 INTRODUCTION

Heavy metal copper is widely used in industrial and agricultural production, such that copper pollution has become one of the most incredibly difficult environmental problems faced by mankind(Fernandes & Henriques, 1991). The effects of copper pollution overburden ecosystems and attract the attention of people worldwide (Ebbs & Kochian, 1997). Currently, the monitoring of heavy metal pollution primarily takes the form of traditional geochemical methods. However, these traditional methods are time consuming, inefficient, and unsuitable to large-scale monitoring. By contrast, vegetation monitoring methods based on remote sensing techniques, with their capacity for wide vision, large amount of information, and rapid dynamic monitoring, have become powerful tools in monitoring heavy metal pollution (Li, 2007). Many scientists have studied the spectral effects of heavy metal pollution on vegetation by monitoring spectral changes (Buschmann, et al., 1998; Jago, et al., 1999; NI, et al., 1997).

Research shows that the status of plant growth and development is an important index of ecosystem pollution and heavy metal-stressed vegetation exhibit changes in the internal structure and spectral properties of their leaves (Liu, et al., 2004; Cho, et al., 2006; Horler, et al., 1980; Sridhar, et al., 2007; Chi, et al., 2006). Li, et al. (2008) proposed that the red edge slope of the copper-stressed leaves of Rhus Chinensis increased from 4.5534 to 8.9475 and the red edge position demonstrated the blue shift phenomenon Chi, et al. (2006) examined the relationships between heavy metal concentration on the one hand and the elevated area of reflectance in the visible wave band, the reduced area in near-infrared wave band, and the blue shift index on the other hand (Qu, et al., 2012). Ren, et al. (2010) extracted the spectral characteristics of contaminated paddy plants and identified the sensitive bands by means of correlation analysis and curve fitting of the inverted Gaussian model. Liu et al. detected the stress levels of rice under Zn pollution by analyzing the characteristics of hyperspectral singularity (Liu, et al., 2010). The aforementioned studies used red edge position, vegetation index, sensitive bands, and wavelet transform

Received: 2013-03-29; **Accepted:** 2013-08-29; **Version of record first published:** 2013-09-06

Foundation: National Natural Science Foundation of China (No. 41271348); China Geological Survey Project (No. 121201112030)

First author biography: ZHU Yeqing (1989—), female, master, she majors in Catography and Geography Information System. E-mail: zhuyeqing0307@foxmail.com

Corresponding author biography: QU Yonghua (1971—), male, associate professor. His research interests are basic theory of quantitative remote sensing and application research about geography information system. E-mail: qyh@bnu.edu.cn

method to enhance the o riginal spectral information and to extract the remote sensing spectral diagnosis index of vegetation pollution, thus attaining the goal of monitoring heavy metal pollution by remote sensing technology. However, the parameters above are easily affected by the stage of plant growth because of the complexity of physical and biochemical response mechanisms. Very few studies involve the monitoring of pernicious metals and the spectra of stressed plants (Ren, et al., 2005). As such, the search for a more effective and sensitive diagnostic method of the simple, rapid, and non-destructive monitoring of heavy metal pollution continues to be a focus in the research agenda.

Wheat and lettuce were selected as the experimental subjects in the laboratory experiments on copper treatment. Forty-six groups of copper-treated leaves were measured at four regular periods. Through these measurements, information on the spectral and biochemical components of the leaves and the corresponding scanning electron microscopy images were obtained. Based on the data above, this study uses characteristic bands to discuss the spectral response effects of copper-stressed leaves on different growth stages. The spectral angle was calculated to d etermine the significance of each copper-stressed leaves. This paper provides a theoretical basis and technical support for the diagnosis and monitoring of copper pollution with plant spectra. The leaf structure parameter N of copper-contaminated leaves was calculated based on the PROSPECT model. The inversion values of the leaf structure parameter N explained the spectral abnormality in the near-infrared bands of the copper-treated leaves. The structure parameter N can be used to monitor mild to moderate copper pollution.

2 METHOD AND EXPERIMENT

2.1 Experiment and data collection

Copper is an element indispensable to plant growth. H owever, excessive heavy metal damages the plant. Generally, the concentration of Cu is 35 μg/g in clear soil (first class field), 100 μg/g in slightly polluted soil (second class field), and 4 00 μg/g in severely polluted soil (third class field) (Zhao, et al., 2008). In this study, we conducted a laboratory experiment on copper-stressed wheat and lettuce. We obtained information on the spectral and biochemical components of the leaves and the corresponding Scanning Electron Microscopy (SEM) images. F inally, we constructed an integrated data set on copper-polluted plants based on the experiment.

Wheat and lettuce were selected as the experimental subjects in the laboratory experiments on copper treatment. The seeds were sown in impermeable plastic pots, each of which c ontained approximately 10 kg of potting mix. The plants were kept in an enclosed area outdoors. They were supplied with d istilled water daily. To simulate heavy metal copper contamination in the soil, the soil was treated with copper sulfate solutions. Ten treatments, including a control group, were designed, with 25 mg/kg, 50 mg/kg, 100 mg/kg, 200 mg/kg, 400 mg/kg, 800 mg/kg, 1600 mg/kg, 3200 mg/kg, and 4800 mg/kg of c opper s ulfate solution respectively. Each treatment was tested three times in parallel.

The spectrum curve ofthe vegetation in its near-infrared band was primarily influenced by the leaf's internal structure, which shows significant abnormality when polluted by copper (Liu, et al., 2010). Therefore, we obtained SEM images of the copper-treated leaves to observe and verify the changes in the leaf's internal structure caused by copper pollution. Forty-six groups of copper-treated leaves were measured at four regular periods. The specific process of data collection is as: (1) We c ollected the reflectance spectra of the leaves. (2) We obtained SEM images. (3) We measured leaf biochemical and copper c ontamination using the laboratory method.

The measurement of leaf reflectance spectra adopts vim measuring method. The reflectance spectra are collected with an ASD Fieldspec3 Spectroradiometer (Analytical Spectral Devices, Boulder, CO, USA) with a wavelength range of 350 nm to 2 500 nm and a spectral resolution of 1 nm. The spectrometer is equipped with a blade clamping device (Unit 1539 Plant Probe, Model A122317). The reflectance spectra of wheat during the jointing and booting stages were measured using the ASD spectrometer coupled with an integrating sphere (Li-1800S). Therefore, the measured reflectance ranges from 300 nm to 1 100 nm, a range that incorporates that of the integrating sphere. For our measurements, we selected three representative leaves from each plant and the average number was set to twenty.

Leaf samples from plants grown in the control soil were collected and prepared for SEM. The samples were frozen and immediately fixed in 2% glutaraldehyde in a 0. 1 M potassium phosphate buffer (pH = 7. 2). All of the materials were maintained at 4℃ and were observed with an SEM, KYKY-EM 3200, with a resolution better than 6 nm. All the observations were completed in two weeks.

The biochemical components were measured using chemical methods. Through chemical analysis, we obtained the chlorophyll, water, dry matter, and copper ion content. Chlorophyll is not soluble in water, but is soluble in organic solvent. Therefore, chlorophyll was extracted from the copper-treated leaves using 80% acetone. To measure the dry matter and water content, the harvested leaves were heated at 105℃ for 30 minutes and were then dried at 70℃ in an oven to achieve a constant weight. The leaf samples (approximately 0. 5 g) were d igested with concentrated nitric acid and hydrochloric acid. The digested solution was filtered, and the copper concentration was then analyzed using atomic absorption spectrophotometry (Optima 2100 DV inductively coupled plasma emission spectrometer, USA PerkinElmer Company).

2.2 Determination of spectral features

This paper uses seven characteristic bands to determine if significant spectral changes occurred in the copper-stressed leaves in different growth periods. The seven characteristic bands and the corresponding calculation method are shown in Table 1.

To determine the spectral significance of each sample, we calculated the spectral angle between the mean reflectance spectraof the given sample and the mean reflectance spectra of the control plants. The spectral angle was calculated at six spectral regions. The six spectral regions are shown in Table 1. We calculated the spectral angle through Eq. (1).

$$\theta = \arccos\left[\frac{\sum\left(R_{\text{control}}(i) \times R_{\text{stress}}(i)\right)}{\left|R_{\text{control}}(i)\right| \times \left|R_{\text{stress}}(i)\right|}\right] \quad (1)$$

where $i = 1, 2, 3, \cdots, n$ θ is the spectral angle, $R_{\text{control}}(i)$ is the reflectance value of the control leaves at wavelength i, and $R_{\text{stress}}(i)$ is the reflectance value of the copper-stressed leaves at wavelength i.

Table 1 Seven characteristic bands and spectral angles

Characteristic bands		Spectral angles		
Band names	Calculation method	Band range/nm	Band intervals/nm	Explanations
Violet trough	Wavelength of the minimum value of the reflectance from 382 nm to 500 nm	400—2500	5	The full spectral angle
Blue edge	Wavelength of the maximum value of the first-order derivative of the reflectance from 450 nm to 550 nm	400—716	4	The spectral angle focused on pigments
Green crest	Wavelength of the maximum value of the reflectance from 500 nm to 600 nm	717—975	3	The spectral angle focused on the red edge
Yellow edge	Wavelength of the minimum value of the first-order derivative of the spectrum from 550 nm to 650 nm	976—1265	17	The spectral angle focused on water content
Red trough	Wavelength of the minimum value of the spectrum from 600 nm to 720 nm	1266—1770	3	The spectral angle focused on water content
Red edge	Wavelength of the maximum value of the first-order derivative of the reflectance from 670 nm to 780 nm	1771—2500	3	The spectral angle focused on water content
Infrared shoulder	Wavelength of the maximum value of the reflectance from 750 nm to 950 nm			

$\left|R_{\text{control}}(i)\right|$ and 0 $\left|R_{\text{stress}}(i)\right|$ can be calculated through Eq. (2).

$$\left|R_{\text{control}}(i)\right| = \sqrt{\left(\sum\left(R_{\text{control}}(i) \times R_{\text{control}}(i)\right)\right)}$$
$$\left|R_{\text{stress}}(i)\right| = \sqrt{\left(\sum\left(R_{\text{stress}}(i) \times R_{\text{stress}}(i)\right)\right)} \quad (2)$$

Additionally, n can be calculated by

$$n = \frac{\lambda_{\max} - \lambda_{\min}}{\delta} \quad (3)$$

where $\lambda_{\max}$ is the upper bond of the spectral bands, $\lambda_{\min}$ is the lower bond of the spectral bands, and δ is the band interval (Dennison, et al., 2004).

If the angle exceeded a threshold for any spectral range, the spectrum was consideredas exhibiting significant spectral changes. The threshold was computed through Eq. (4).

$$\varepsilon_x = \arccos\left[\frac{\sum\left(R_{\text{control\_}x}(i) \times \bar{R}(i)\right)}{\left|R_{\text{control\_}x(i)}\right| \times \left|\bar{R}(i)\right|}\right]$$
$$\varepsilon = \frac{\sum_{x=1}^{q}\varepsilon_x}{q} \quad (4)$$

where $R_{\text{control\_x}}(i)$ is the reflectance value of the measurement x of the control group leaves, $\bar{R}(i)$ is the mean reflectance value of the control group leaves at wavelength i, and q is the total number of measurements. In conclusion, the threshold values for each spectral range were determined by calculating the difference between the reflectance value of a single measurement and the mean reflectance value of the control sets for each species.

2.3 Determination of spectral structure parameter *N* of copper-treated leaves

Leaf structure is described by a parameter that represents the delaminating phenomenon of leaf interior space in the leaf radiative transfer model. Leaf structure parameter is an immeasurable parameter and can only be obtained by inversion. The PROSPECT model is used to calculate it. Based on radiative transfer theory, PROSPECT describes the optical properties of a leaf from 400 nm to 2500 nm with a minimum number of p arameters to facilitate its inversion.

A leaf isassumed to be composed of a pile of N homogeneous layers separated by $N-1$ air spaces. The non-diffuse character of the incident beam concerns only the top of the pile. Inside the leaf, the light flux is assumed to be isotropic. The final equation of the PROSPECT model requires four parameters: α, N, n, and k (Jacquemoud & Baret, 1990).

The determination of N requires the refractive index. In our case, the refractive index was set to 1.45. Increasing or decreasing the value of the refractive index did not change the results. For the copper-treated dataset, we chose the three wavelengths corresponding to the three maximum reflectances from 800 nm to 1200 nm to obtain the inversion value of N_{Cu}. The cost function is

$$J\left(N_{\text{Cu}}, k\left(\lambda_{\max 1}\right), k\left(\lambda_{\max 2}\right), k\left(\lambda_{\max 3}\right)\right) = \sum_{i=1}^{3}\left(R_{\text{mes}}\left(\lambda_{\max i}\right) - R_{\text{mod}}\left(\lambda_{\max i}\right)\right)^2 \quad (5)$$

where N_{Cu} is the structure parameter of the copper-stressed leaves, $k(\lambda_{\max i})$ is the corresponding specific absorption coefficients at $\lambda_{\max i}$, $R_{\text{mes}}(\lambda_{\max i})$ is the measured reflectance at $\lambda_{\max i}$, and $R_{\text{mod}}(\lambda_{\max i})$ is the simulated reflectance at $\lambda_{\max i}$.

3 DATA PROCESSING AND ANALYSIS

3.1 The reflectance spectra of copper-treated leaves

The corresponding leaf reflectance spectra of copper-treated wheat and lettuce are shown in Fig. 1 and Fig. 2. The germination rate of lettuce is virtually zero when the stress concentration

is 1600 μg/g, 3200 μg/g, and 4800 μg/g. In our experiment, we measured the leaf reflectance spectra of only five groups of c opper-treated l ettuce. Compared with healthy leaves, the reflectance spectra of copper-stressed leaves either increased or d ecreased. Among the full band intervals, the reflectance values from 800 nm to 1 300 nm showed the most significant difference. This difference is not regular, but is related to plant species and growth period. For example, the reflectance value of copper-treated wheat in the seeding and heading stages is less than that of healthy wheat. However, the above mentioned regulation does not manifest in the jointing and filling stages. The reflectance spectra of two leaves of the copper-treated lettuce is less than that of healthy leaves in the visible and mid-infrared band ranges, but is greater than that of healthy leaves in the near-infrared range. The reflectance spectra of six and eight leaves of c opper-treated lettuce is less than that of healthy lettuce. In c onclusion, distinguishing b etween copper-treated leaves and healthy leaves directly through reflectance spectra is not easy.

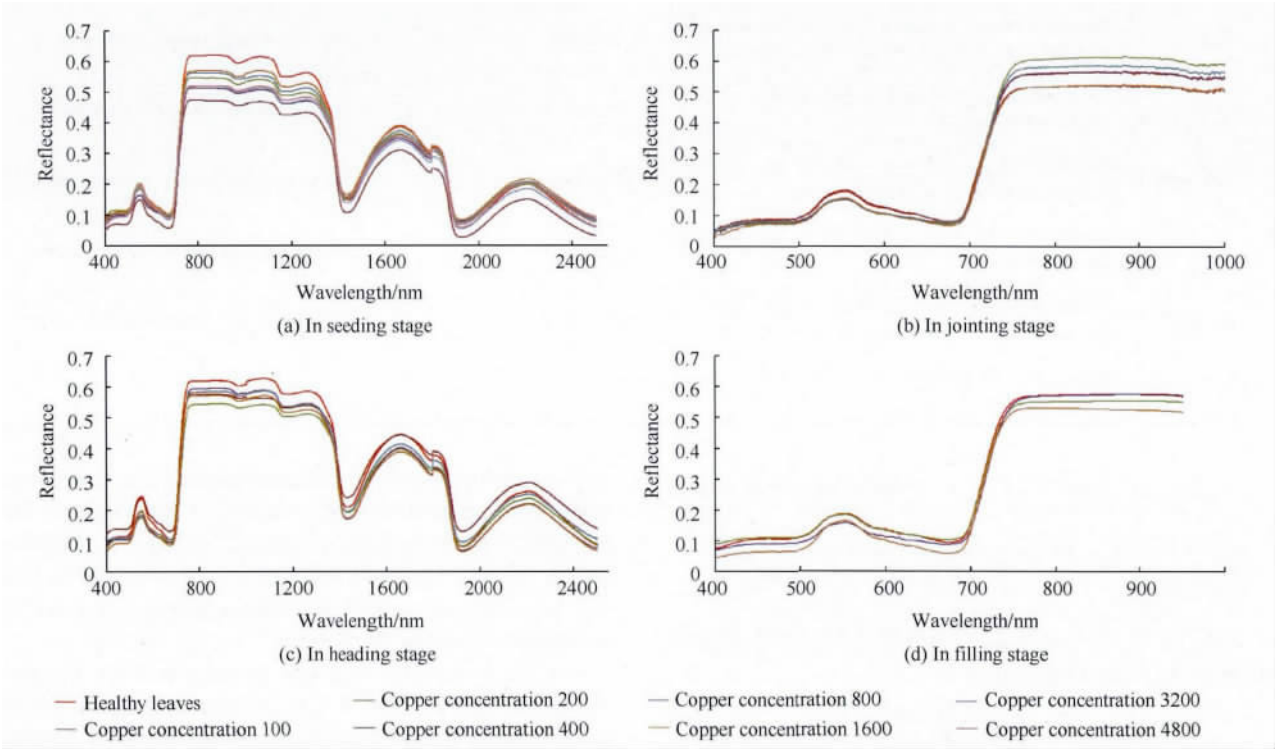

Fig. 1 Reflectance spectra of wheat leaves

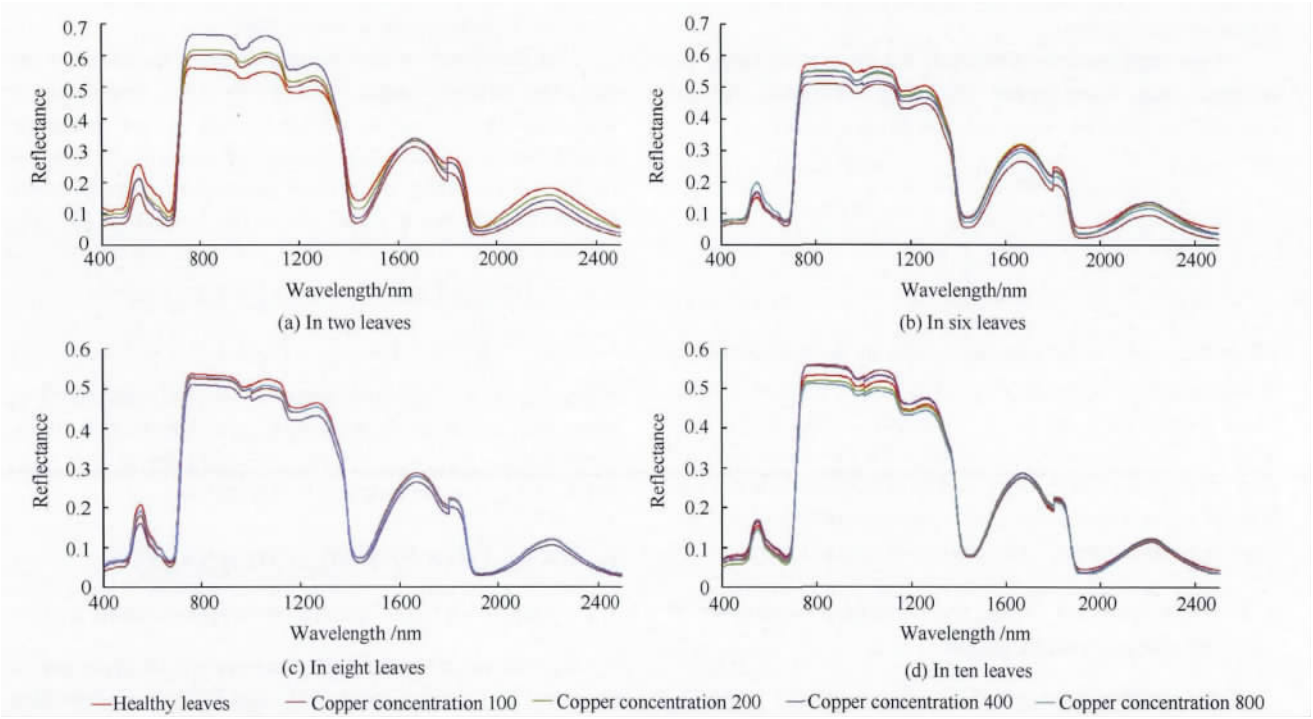

Fig. 2 Reflectance spectra of lettuce leaves

3.2 The analysis of reflectance spectra of copper-treated leaves

Previous research shows that the copper content in soil and plant leaves has the same varying trend and significant positive correlation (Chi, et al., 2005). In other words, the copper content in plant leaves increases with copper content in soil (Liu, et al., 2007). Fig. 3 shows the seven characteristic bands of wheat. The horizontal axis represents the copper content of leaves and the vertical axis represents the wavelength. The band position of the violet trough, blue edge, green crest, yellow edge, and red trough of wheat do not change significantly with an increase in the c opper content of leaves throughout the four growth periods. The maximum deviation is less than 3 nm. The red edge position of the seeding, jointing, heading, and filling stages shift from 7 13 nm to 719 nm, 708 nm to 711 nm, 714 nm to 704 nm, and 712 nm to 707 nm, respectively, with an increase in the copper content of leaves. The infrared shoulder shows an obvious red shift in the seeding and jointing stages and a significant blue shift in the heading and filling stages.

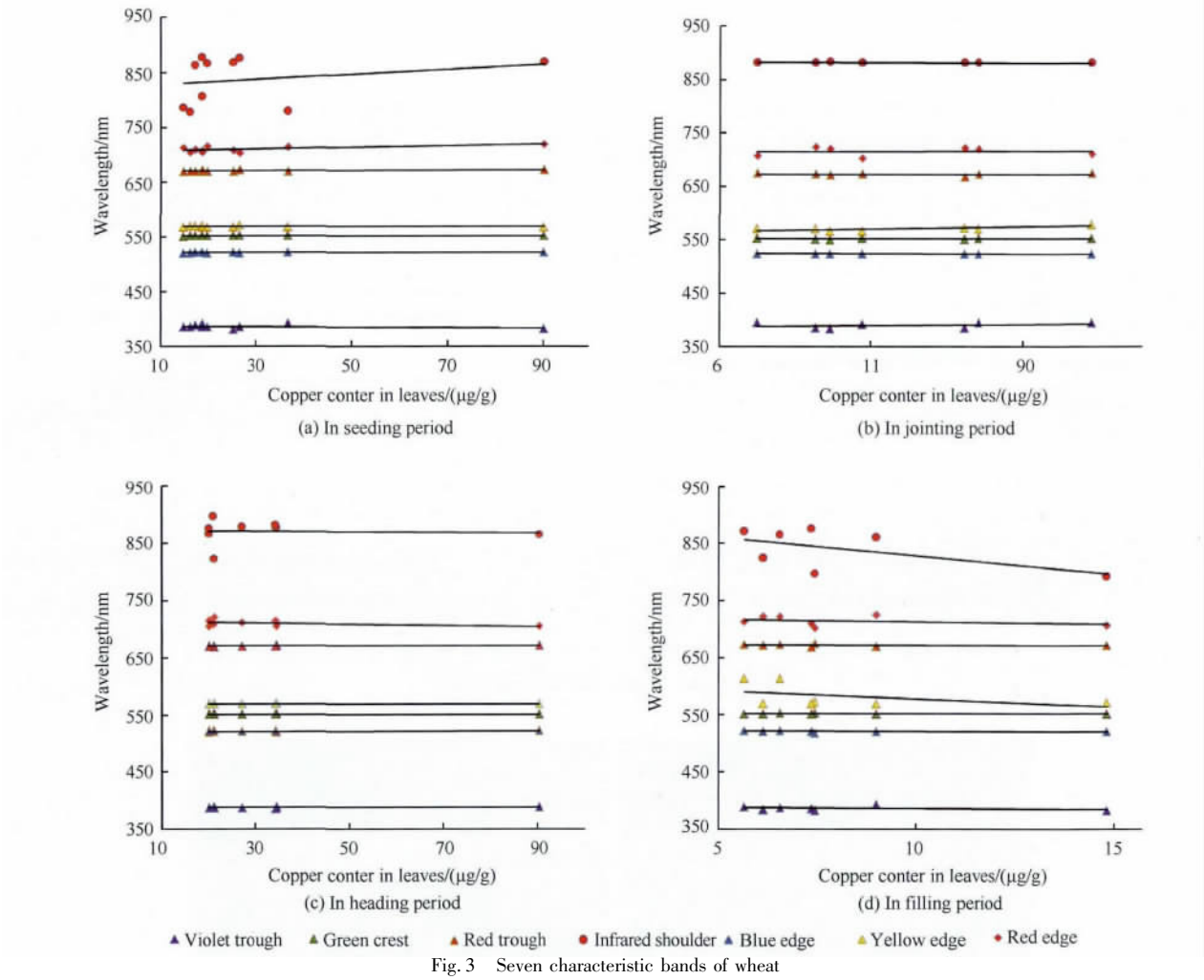

Fig. 3 Seven characteristic bands of wheat

Fig. 4 shows the seven characteristic bands of lettuce. The band position of the violet trough, blue edge, green crest, yellow edge, and red trough of wheat does not change significantly with an increase in the copper content of leaves throughout the four growth periods. The maximum deviation is less than 3 nm. The red edge position of two leaves, six leaves, eight leaves, and ten leaves shift from 701 nm to 707 nm, 713 nm to 708 nm, 702 nm to 708 nm, and 705 nm to 711 nm, respectively, with an increase in the copper content of leaves. The infrared shoulder shows an obvious blue shift in the two and six leaves and a significant red shift in the eight and ten leaves.

Fig. 5 shows the SEM images of the transverse section of the copper-treated leaves. The internal structure of the leaf b ecomes more disordered as the copper concentration of the leaf increases. As the metal concentration increases, the following cellular changes occur: the decomposition of the upper epidermal cells, the shrinking of the mesophyll cells, and the disintegration of the vascular bundle.

Fig. 6 shows the relationship between the reflectance values of the infrared shoulder and the leaf's internal structure parameter N for both wheat and lettuce. The spectral characteristics in the near-infrared band depend on internal leaf structure (Zhao, 2003). Research shows that healthy leaves have N values between 1.5 and 2.5, and a larger N indicates a more disorganized internal structure (Jacquemoud & Baret, 1990). The results shown in Fig. 6 indicate that N_{Cu} ranges from 3.3 to 4.2. Therefore, based on the inversion results, the copper-stressed leaves have a more disorganized internal structure than do the

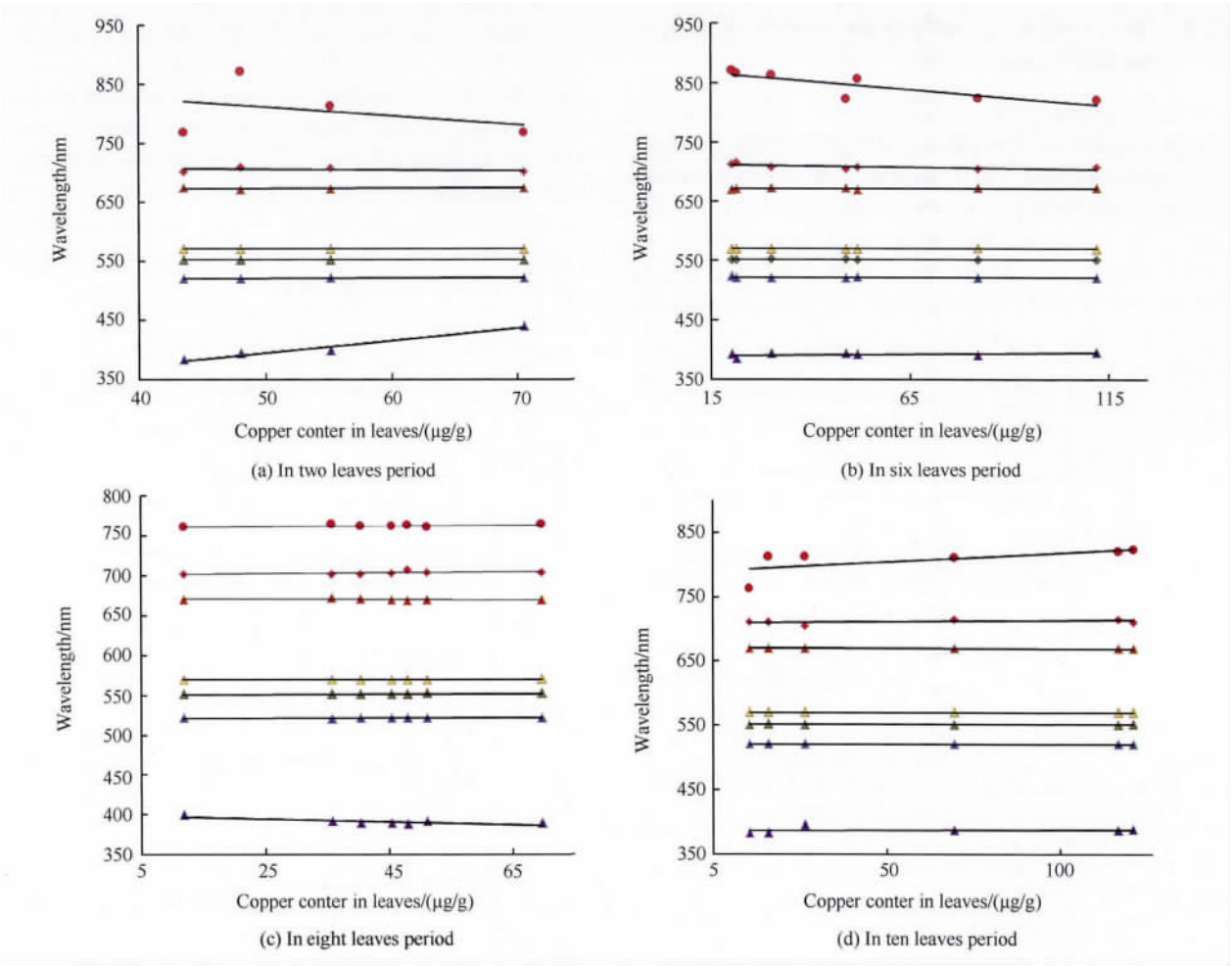

Fig. 4 Seven characteristic bands of lettuce

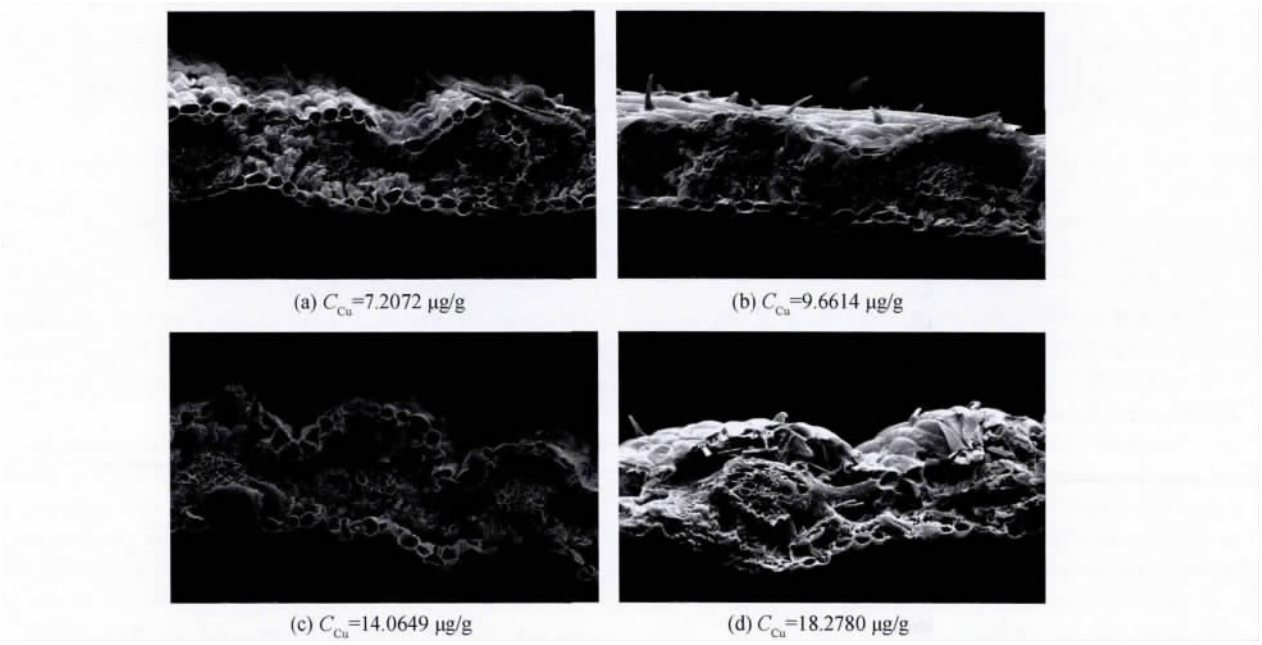

Fig. 5 SEM images of the transverse section of wheat

unstressed leaves. This conclusion coincides with the results of the SEM images (Fig. 5). The results interpret the spectral differences between the near-infrared band of the copper-treated leaves and that of the healthy leaves. Leaf reflectance spectra can be used to obtain the inverse of a leaf's internal structure parameter N and then to monitor heavy metal pollution based on N v alues. An N value greater than 2.5 indicates the obvious variation of a leaf's internal structure. As such, the plants are polluted by heavy metal. The reflectance values of copper-treated leaves in the infrared shoulder exhibit a significant positive linear correlation with the leaf's internal structure parameter. The linear relationship between N and the reflectance value of the red shoulder was fitted with a correlation coefficient of 0.978.

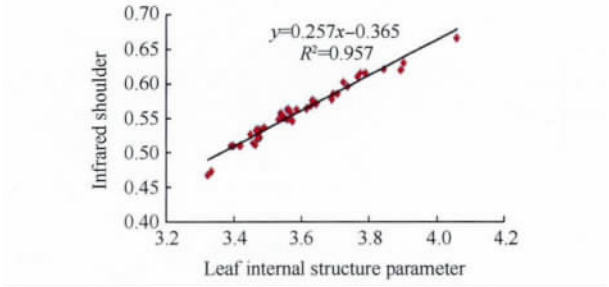

Fig. 6 Relationship between the leaf internal structure parameter and the reflectance values of copper-treated leaves atthe infrared shoulder

The red edge is the main reflectance feature of the copper-treated leaves in the visible range. It shows regular changes in one growth period. Studies show that the red edge position is affected mainly by the leaf's internal structure and chlorophyll content (Liang, et al., 2009). When the value of the leaf structure parameter is increased, the red edge changes toward the short wave (Liang, et al., 2009). Many complex factors lead to a "red shift" phenomenon at the red edge position, but one important factor is the replacement of chlorophyll by xanthophyll, which causes a content decrease in the leaves (Horler, et al., 1983). Wheat has vigorous vegetation growth in the seeding and jointing stages, both of which constitute an important period of chlorophyll accumulation. Copper stress results in a decrease in chlorophyll and an increase in xanthophyll. Therefore, copper-treated wheat in the seeding and jointing stages demonstrates a "red shift" phenomenon at the red edge position. This is also the reason why lettuce presents "red shift" at the red edge position during the periods when it has eight and ten leaves. The heading and filling stages are an important period of reproductive growth. During these periods, the red edge position is affected mainly by the leaf's internal structure. Copper stress leads to a more disorganized leaf internal structure and a larger leaf structure parameter. Therefore, copper-treated wheat in the heading and filling stages demonstrates a "blue shift" phenomenon at the red edge position. This is also the reason why lettuce exhibits a "blue shift" at the red edge position during the periods when it has two and six leaves.

3.3 Analysis of spectral angle of copper-treated leaves

Fig. 7 compares the spectral angles and threshold values of wheat and Brassica chinensis in six specific spectral regions. The horizontal axis represents the growth period of the experimental samples, and the vertical axis represents the corresponding spectral angles. As shown in Fig. 5, more than 90% of the copper-treated leaves exhibit significant spectral changes compared with the control samples across the full spectral range (400—2500 nm), 77% of the copper-stressed leaves show s ignificant spectral changes in the visible region focusing on p igments (400—716 nm), 76% of the copper-treated leaves e xhibit obvious spectral changes in the region focusing on the red edge (717—975 nm), and 87% of the copper-treated leaves show significant spectral changes in the three regions associated with water content. The statistical results for the spectral angles in the six band regions above show that more than 84% of the copper-stressed leaves have a spectral angle greater than the threshold value. These results indicate that more than 84% of the copper-treated leaves have significant spectral differences.

The reflectance spectra of leaves are affected mainly by the chlorophyll content in the visible region, influenced by the leaf's internal structure in the near-infrared spectrum, and determined by water content in the mid-infrared bands (Jacquemoud & Baret, 1990). Previous studies show that the transportation of copper ion in plant cells is related to the copper concentration inside or outside the cell and is conducted by a specific receptor. If plants absorb too much outer copper, they tend to store more water by reducing water transpiration to decrease copper ion concentration. Serious copper pollution affects the normal physiological metabolic activity of chlorophyll. The leaf becomes thicker and the surface area becomes smaller. The leaf intercellular structure diminishes and leaf turns yellow (Gou, 2010; Wang & Wang, 2005). This phenomenon theoretically explains the spectral variations of copper-treated leaves.

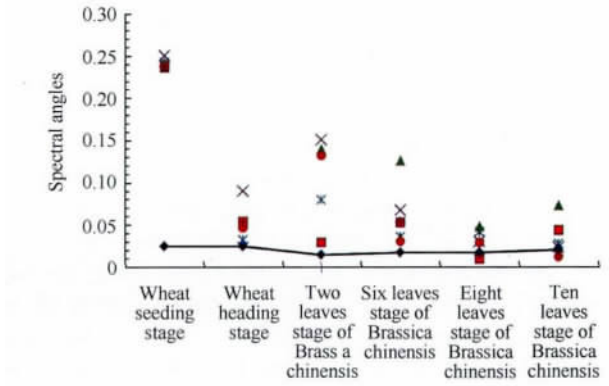

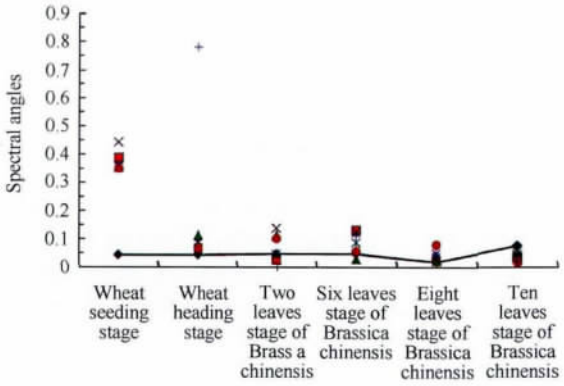

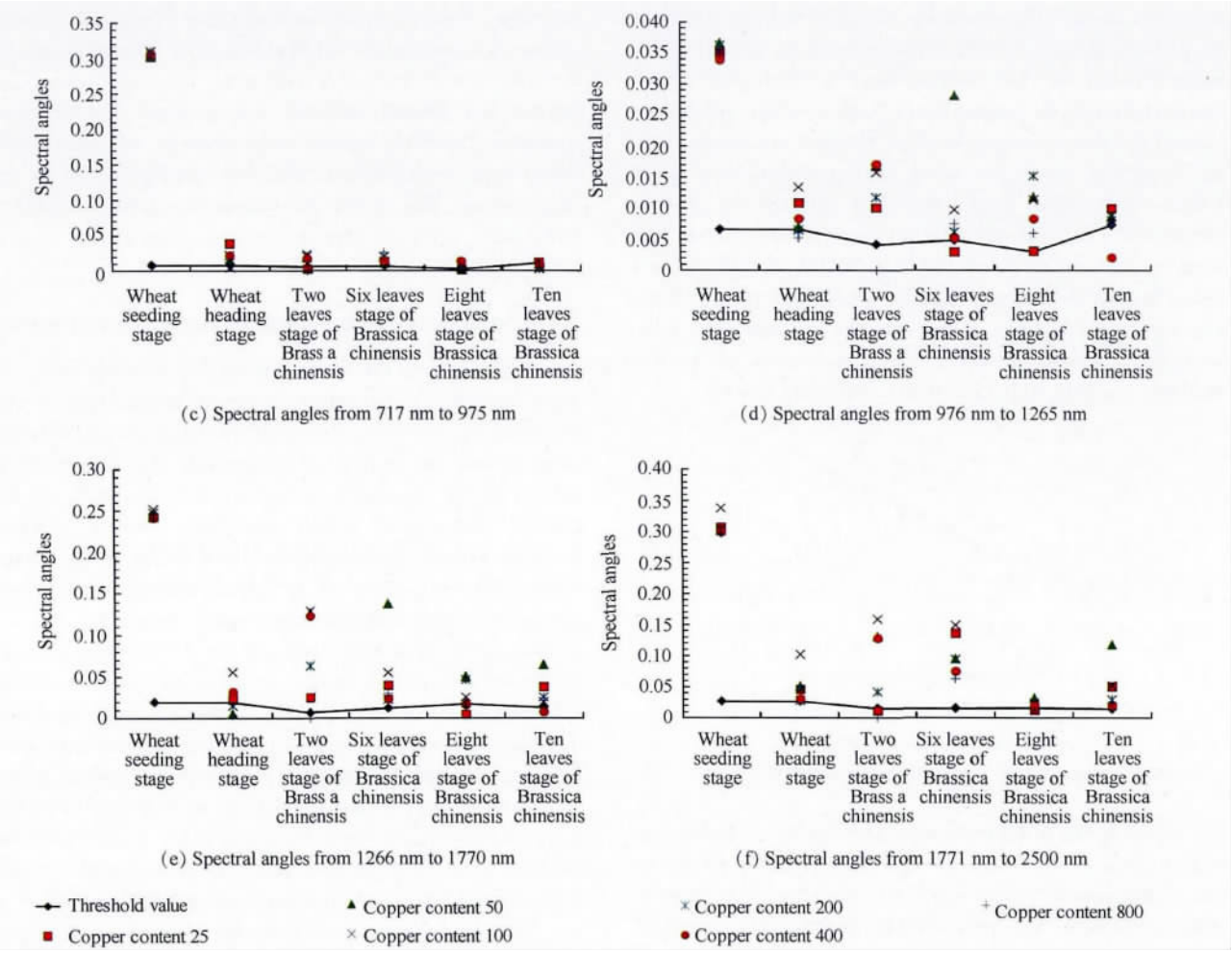

Fig. 7 Spectral angles calculated at six spectral regions

Spectral angle is a general method of detecting copper pollution. Unrelated to growth period and plant species, it needs only a simple comparison with the threshold values. On the one hand, the spectral angle is very sensitive to spectral variations from 400 nm to 2500 nm. On the other hand, plants in general are very sensitive to copper toxicity, displaying metabolic disturbances and growth inhibition, with the copper content in the tissues only slightly higher than the normal level (Fernandes & Henriques, 1991). Therefore, the spectral angle can be used to detect slight to moderate copper pollution. This method is sensitive to copper pollution and does not result in destructive sampling.

4 CONCLUSION

This study investigated the spectral changes in copper-polluted leaves using seven spectral signatures and the spectral angle method. Wheat and lettuce, selected as the experimental subjects, were cultivated in copper-polluted soil. The leaf spectra reflectance from 400 nm to 2500 nm and the SEM of ten copper treatment groups were measured at four regular periods. By theoretical and statistical analysis, we draw the following conclusions: (1) The differences between copper-stressed leaves and healthy leaves are irregular and related not only to growth period but also plant species. (2) The copper-polluted leaves and healthy leaves can be distinguished at the red edge and infrared shoulder, but the violet trough, blue edge, yellow edge, green crest, and red trough can also be used to describe the spectral differences of copper-treated leaves in the visible region. (3) The leaf structural parameter of copper-polluted leaves is larger than that of healthy leaves. It indicates a more disorganized internal leaf structure. The linear relationship between N and the reflectance value of the red shoulder was fitted using a correlation coefficient of 0.978. (4) Spectral angle is a general method of detecting copper pollution and it is not related to growth period and plant species. It needs only a simple comparison with the threshold values. It is very sensitive to spectral variations from 400 nm to 2500 nm.

This research looks into the qualitative relationship between reflectance spectra changes of the copper-treated leaves and the spectral characteristics of their internal structure. Future research should further explore the relationship in quantitative terms and conduct more comprehensive laboratory cultivation experiments. We can study the internal mechanisms of spectral changes caused by copper pollution using laboratory experiments.

Acknowledgements: Our laboratory experiment was supported by Professor Ji Shengdong and associate professor Liu Haiying of Henan Normal University. We thank professor Wang Jindi of Beijing Normal University for providing constructive advice and guidance during the whole research.

REFERENCES

Chi G Y, Liu X H, Liu S H and Yang Z F. 2005. The relationships between heavy metals pollution and spectral characteristics of Miscanthus floridulus in Dawu River basin. Ecology and Environment, 14(4): 549 - 554

Chi G Y, Liu X H, Liu S H and Yang Z F. 2006. Studies of relationships between Cu pollution and spectral characteristics of TritiZnm Aestivum L. Spectroscopy and Spectral Analysis, 26(7): 1272 - 1276

Buschmann C, Lichtenthaler H K. 1998. Principles and characteristics of multi-colour fluorescence imaging of plants. Journal of Plant Physiology, 152(2): 297 - 314.

Cho M A, Skidmore A K and Atzberger C. 2006. Towards red-edge positions less sensitive to canopy biophysical parameters using Prospect-Sailh simulated data, ISPRS

Dennison P E, Halligan K Q and Roberts D A. 2004. A comparison of error metrics and constraints for multiple endmember spectral mixture analysis and spectral angle mapper. Remote Sensing of Environment, 93(3): 359 - 367 [DOI: 10.1016/j.rse.2004.07.013]

Ebbs S D and Kochian L V. 1997. Toxicity of zinc and copper to Brassica species: implications for phytoremediation. Journal of Environmental Quality, 26(3): 776 - 781

Feret J B, François C, Asner G P, Gitelson A A, Martin R E, Bidel L P R, Ustin S L, le Maire G and Jacquemoud S. 2008. PROSPECT-4 and 5: Advances in the leaf optical properties model separating photosynthetic pigments. Remote Sensing of Environment, 112(6): 3030 - 3043 [DOI: 10.1016/j.rse.2008.02.012]

Fernandes J and Henriques F. 1991. Biochemical, physiological, and structural effects of excess copper in plants. The Botanical Review, 57(3): 246 - 273 [DOI: 10.1007/BF02858564]

Gou J Y. 2010. Copper Stress on Purpurea Growth and Development. Chengdu: Sichuan Normal University

Horler D, Dockray M and Barber J. 1983. The red edge of plant leaf reflectance. International Journal of Remote Sensing, 4(2): 273 - 288 [DOI: 10.1080/01431168308948546]

Horler D N H, Barber J and Barringer A R. 1980. Effects of heavy metals on the absorbance and reflectance spectra of plants

Jacquemoud S and Baret F. 1990. PROSPECT: a model of leaf optical properties spectra. Remote Sensing of Environment, 34(2): 75 - 91 [DOI: 10.1016/0034 - 4257(90)90100 - Z]

Jago R A, Cutler M E J and Curran P J. 1999. Estimating canopy chlorophyll concentration from field and airborne spectra. Remote Sensing of Environment, 68(3): 217 - 224.

Li N. 2007. The Spectral and Image Characteristics of Vegetation in the Press of Heavy Metal. Qingdao: Shandong University of Science and Technology

Li Q T, Yang F J, Zhang B, Zhang X and Zhou G Z. 2008. Biogeochemistry responses and spectral characteristics of Rhus Chinensis Mill under heavy metal contamination stress. Journal of Remote Sensing, 12(2): 284 - 290

Liang S Z, Shi P, Ma W D, Xing Q G and Yu L J. 2010. Relational analysis of spectra and red-edge characteristics of plant leaf and leaf biochemical constituent. Chinese Journal of Eco-Agriculture, 18(4): 804 - 809

Liu M L, Liu X N, Li T and Xiu L N. 2010. Analysis of hyperspectral singularity of rice under Zn pollution stress. Transactions of the Chinese Society of Agricultural Engineering, 26(3): 191 - 197

Liu S H, Liu X H, Hao J, Chi G Y and Cui B S. 2008. A research about cabbage spectral response to copper stress, Scientia Sinica Techologica, 51(2): 202 - 208

Liu S W, Gan F P and Wang W S. 2004. The application of hyperion data to extracting contamination information of vegetation in the dexing copper mine, Jiangxi Province, China. Remote Sensing for Land and Resources, 59(1): 6 - 10, 31

Ni J, Wu J Y. 1997. Prospection of hidden depositusing spectral reflectance of plant leaves surface, Chinese Bulletin of Botany, 14(1): 36 - 40

Qu Y, Liu S H and Li X W. 2012. A novel method for extracting leaf-level solar-induced fluorescence of typical crops under Cu stress. Spectroscopy and Spectral Analysis, 32(5): 1282 - 1286

Ren H Y, Pan J J and Zhang J B. 2005. Hyper-spectral application to monitoring plumbum pollution of vegetation. Remote Sensing Information, (3): 34 - 38

Ren H Y, Zhuang D F, Pan J J, Shi X Z, Shi R H and Wang H J. 2010. Study on canopy spectral characteristics of paddy polluted by heavy metals. Spectroscopy and Spectral Analysis, 30(2): 430 - 434

Sridhar M B B, Han F X and Diehl S V. 2007. Monitoring the effects of arsenic and chromium accumulation in Chinese brake fern (Pteris vittata), International Journal of Remote Sensing, 28(5): 1055 - 1067

Tan Q, Zhao Y C, Tong Q X and Zheng L F. 2001. Vegetation spectral feature extraction model. Remote Sensing Information, 1(1): 14 - 18

Wang J and Wang S J. 2005. The sources and crops effect of heavy metal elements of contamination in soil. Journal of Guizhou Normal University (Natural Science), 23(2): 113 - 120

Zhao J N. 2008. Effect of Soil Copper Contamination on Growth And Development of Rice. Yangzhou: Yangzhou University

Zhao Y S. 2003. Theory and Method of Remote Sensing Application Analysis. Beijing: Science Press

重金属铜污染植被光谱响应特征研究

朱叶青[1,2]，屈永华[1,2]，刘素红[1,2]，陈圣波[3]

1. 北京师范大学 遥感科学国家重点实验室 遥感与地理信息系统研究中心，地理学与遥感科学学院，北京 100875;
2. 环境遥感与数字城市北京市重点实验室，北京 100875;
3. 吉林大学 地球探测科学与技术学院，吉林 长春 130026

摘 要: 重金属铜污染植被的反射光谱特性会发生明显改变。在本研究中,采用不同程度的铜污染土壤作为培养基质,选择春小麦、上海青两种农作物进行铜胁迫实验,获取了 4 个不同生育期、10 个不同铜污染强度下的植被叶片的反射光谱,并采用铜污染叶片 7 个特征波段和光谱角的方法研究了铜污染叶片的光谱特征。结果表明,铜污染叶片光谱差异与作物时期和作物类型有关,可以采用叶片光谱角描述铜污染叶片与健康叶片的光谱差异。该方法只需与阈值做简单的比较,方法简便易行,而且对轻度及重度铜污染十分敏感。叶片光谱辐射传输模型反演结果表明铜污染叶片内部结构参数 N 明显变大,这也证明了铜污染使叶片内部结构更加散乱无序。在此基础上进一步建立了 N 与红肩处反射率值的线性关系,相关系数为 0.978。本文为铜污染叶片光谱反射模型的建立提供了初步的数据基础与理论支持。

关键词: 重金属污染,叶片光谱,特征波段,光谱角,PROSPECT 模型

中图分类号: X87 **文献标志码**: A

引用格式: 朱叶青,屈永华,刘素红,陈圣波. 2014. 重金属铜污染植被光谱响应特征研究. 遥感学报,18(2): 335 -352

Zhu Y Q, Qu Y H, Liu S H and Chen S B. 2014. Spectral response of wheat and lettuce to copper pollution. Journal of R emote Sensing, 1 8(2): 335 -352 [DOI: 10.11834/jrs.20143073]

1 引 言

随着重金属铜在工业和农业生产中的广泛应用,重金属铜污染已经成为人类面临的非常棘手的环境问题(Fernandes 和 Henriques,1991)。超负荷铜对生态系统的污染已经引起人们的高度重视,并受到世界各国的广泛关注(Ebbs 和 Kochian 等,1997)。目前重金属污染监测主要依赖传统的地球化学方法,该方法费时、费力,不适合大范围监测。而基于遥感技术的植被光谱监测方法,以其视野宽、信息量大和快速动态监测的优点,成为重金属污染监测及识别的有力工具(李娜,2007)。许多学者已经致力于研究重金属污染的植被光谱效应,旨在通过重金属胁迫植被的光谱特征变化来监测重金属污染(Buschmann 等,1998; Jago 等,1999; 倪健 等,1997)。

研究表明,植物的生长发育状况是指示生态系统污染的一项重要指标(刘圣伟 等,2004),而且重金属污染植被的反射光谱特性会发生明显改变(Cho 等,2006; Horler 等,1980; Sridhar 等,2007; 迟光宇 等,2006)。李庆亭等人(2008)提出受到铜胁迫的盐肤木叶片的红边斜率从 4.5534 增加到 8.9475,红边发生 10—20 nm 的蓝移; 迟光宇等人(2006)建立了可见光反射率升高面积 A_1、近红外降低面积 A_2 和红边"蓝移"指数 S 与重金属胁迫强度的关系,取得了理想的结果(瞿瑛 等,2012); 任红艳等人(2010)通过曲线模拟和统计分析提取了与水稻冠层叶片重金属含量变化极显著相关的反射光谱特征,并进一步研究其与重金属污染水稻叶片的相关关系; 刘美玲等人(2010)尝试利用小波变换对受污染胁迫的水稻光谱奇异性特征进行分析,从而达

收稿日期: 2013-03-29; 修订日期: 2013-08-29; 优先数字出版日期: 2013-09-06

基金项目: 国家自然科学基金(No. 41271348); 中国地质调查局地质调查工作项目(No. 1212011120230)

第一作者简介: 朱叶青(1989—),女,硕士,专业为地图学与地理信息系统。E-mail: zhuyeqing0307@foxmail.com

通信作者简介: 屈永华(1971—),男,副教授,主要从事定量遥感基础理论与地理信息系统应用方面的研究。E-mail: qyh@bnu.edu.cn

到诊断水稻锌污染状况的目的。上述研究采用红边位置、植被指数、敏感波段和小波变换等方法对原始光谱信息进行变换或增强,提取植物污染胁迫遥感诊断光谱指数,从而达到利用遥感技术监测重金属污染的目的。然而,由于植物生化物理响应机制问题的复杂性,上述参数均受到作物所处时期的影响。而且,无论叶片还是冠层光谱研究,目前比较深入的都是营养元素或者有益元素以及人体必需元素,而对有害金属尤其是重金属污染的叶片冠层光谱监测研究较少(任红艳 等,2005)。因此,寻找一种更为有效且敏感的诊断方法实现快速、简便、非损伤地监测重金属污染一直是该领域的研究热点。

本文进行了室内铜胁迫小麦和上海青实验,获取了小麦和上海青叶片 4 个不同时期的叶片反射光谱信息、扫描电镜照片信息、叶片叶绿素含量、叶片铜含量、叶片干物质含量和叶片水分含量信息,形成了关于重金属铜污染叶片的一套完整数据集。在对数据处理与分析方法中,采用多个特征波段的方法研究了重金属铜污染叶片不同时期的光谱响应效应; 利用不受作物所处时期影响的光谱指数——光谱角的方法(Dennison 等,2004) 对 4 个不同时期重金属铜污染植被叶片 400—2500 nm 波段区间的光谱变化进行分析,从而达到诊断铜污染状况的目的,最终为基于遥感技术的植被光谱监测方法提供了理论依据和技术支持。与此同时,本文基于叶片通用光谱模型——PROSECT 模型反演了重金属污染植被结构参数 N,基于 N 值的反演结果,解释了铜污染叶片近红外谱段的光谱异常出现的原因,研究结果表明该结构参数 N 可被用来监测轻度及中度铜污染。

2 方法和实验

2.1 实验与数据收集

铜(Cu) 是植物生长所必需的元素,但土壤 Cu 浓度过高会给植物生长造成伤害。一般认为,清洁土壤(一级农田) 的 Cu 浓度为 35 μg/g,轻污染土壤(二级农田) 的 Cu 浓度为 100 μg/g,重污染土壤(三级农田) 的 Cu 浓度为 400 μg/g (赵江宁,2008)。本文进行的室内铜胁迫小麦和上海青实验,获取了不同铜污染浓度下小麦和上海青的叶片反射光谱、生化组分含量信息及叶片扫描电镜照片,形成了关于铜污染植被的一套完整的数据集。

栽培试验选取选取“新春 17 号”春小麦和上海青作为实验对象进行培育。该实验采用不透水的花盆做盆栽实验。重金属以硫酸铜溶液的形式采用逐层喷洒,翻土混合的方式加入。每盆装土 10 kg (土壤为未污染菜园土,pH 值为 7.5),花盆内土层实际形成空间为直径 25 cm、深度 18 cm 的圆柱体。按耕层深度 30 cm 计算,施肥每盆的肥料量为 2.20 g,折合为 220 μg/g。试验设置 8 个 Cu 污染浓度梯度,分别为 0、100、200、400、800、1600、3200 和 4800 μg/g,每个浓度设置 3 组平行试验。

植物光谱曲线在近红外波段主要受到叶片结构的影响。重金属污染叶片的光谱曲线在近红外波段出现明显异常(刘美玲 等,2010)。因此,本实验采集了铜污染叶片的扫描电镜照片,用以观察和验证由重金属污染引起的叶片结构的改变。室内铜污染胁迫实验定期采集数据,共获取了 4 个不同时期(小麦: 苗期、拔节期、抽穗期和灌浆期; 上海青: 二叶一心时期、六叶一心时期、八叶一心时期和十叶一心时期) 叶片反射光谱信息、扫描电镜照片、叶片叶绿素含量、叶片铜含量、叶片干物质含量和叶片水分含量信息。数据采集的具体流程为: 首先测量叶片反射光谱,然后利用扫描电镜获取这些叶片的显微照片,最后通过实验室化验方法获取生化组分含量以及叶片铜含量信息。

叶片反射率光谱的测量采用活体测量的方法,用 ASD FieldSpec3 便携式野外光谱仪 (Analytical Spectral Devices, Inc. Boulder, CO , USA) 和叶片夹置器(Unit 1539 Plant Probe, Model A122317) 耦合测量,拔节期和灌浆期小麦叶片反射光谱信息采用 ASD 光谱仪耦合 Li-1800S 积分球的方式测量。其中光谱仪的测量范围是 400—2500 nm,经过重采样之后的光谱分辨率为 1 nm。由于积分球的测量范围为 300—1100 nm,因此拔节期和灌浆期小麦叶片反射光谱的光谱范围较窄。在测量样本叶片光谱时,每株植物选择有代表性的 3 片叶片测量,其中每条波谱平均次数设置为 20 次。

叶片扫描电镜照片的测量采用扫描电镜(型号为 KYKY-EM3200,分辨率优于 6 nm) 完成: 首先冷冻断裂,然后置于 2% 戊二醛固定液(由 0.1 M,pH =7.2 的 PBS 缓冲液配制) 中,以 4℃ 恒温保存,并保证在两周内完成所有样品观测。

叶片铜含量参数测量采用化学分析方法,对采集的叶片进行冲洗、烘干,并经过 HNO_3、$HCLO_4$ 溶液处理后,用原子吸收分光光度计(Optima 2100 DV

电感耦合等离子体发射光谱仪,美国 PerkinElmer 公司生产)测量叶片中的铜含量。叶绿素 a、b 的含量采取丙酮浸泡提取的方法测量。叶片水分含量、干物质含量的测定采用 105℃杀青 30 min 后,在 70℃烘干至恒重分别称量的方法。

2.2 光谱特征计算方法

本文采用 7 个光谱特征波段来分析不同生育期重金属污染植被与健康植被之间的波谱差异。7 个特征波段及其计算方法如表 1 所示(谭倩 等,2001)。

表 1 光谱特征波段和光谱角

光谱特征波段		光谱角		
名称	计算方法	波段区间/nm	波段间隔/nm	说明
紫谷	叶片反射光谱在 382—500 nm 的最小值	400—2500	5	全波段光谱角
蓝边	叶片反射光谱一阶导数在 450—550 nm 的最大值	400—716	4	反映叶绿素影响引起的光谱变化
绿峰	叶片反射光谱在 500—600 nm 的最大值	717—975	3	反映红边变化引起的光谱差异
黄边	叶片反射光谱一阶导数在 550—650 nm 的最小值	976—1265	17	反映由于叶片中水分含量变化引起的光谱差异
红谷	叶片反射光谱在 600—720 nm 的最小值	1266—1770	3	反映由于叶片中水分含量变化引起的光谱差异
红边	叶片反射光谱一阶导数在 670—780 nm 的最大值	1771—2500	3	反映由于叶片中水分含量变化引起的光谱差异
红肩	叶片反射光谱在 750—950 nm 的最大值			

除此之外,采用光谱角的方法对小麦和上海青 4 个生育期的铜污染叶片进行分析,检验铜污染叶片光谱特性是否发生了明显变化,从而达到检测铜污染的目的。光谱变化显著程度的检验通过比较铜污染叶片反射光谱均值与控制组叶片反射光谱均值实现。本研究在表 1 所示 6 个波段区间计算光谱角,光谱角的计算公式如下:

$$\theta = \arccos\left[\frac{\sum\left(R_{\text{control}}(i) \times R_{\text{stress}}(i)\right)}{\left|R_{\text{control}}(i)\right| \times \left|R_{\text{stress}}(i)\right|}\right] \quad (1)$$

式中,$i=1,2,3,\cdots,n$,θ 为光谱角,$R_{\text{control}}(i)$ 为控制组叶片在波长 i 处的反射率,$R_{\text{stress}}(i)$ 为胁迫组叶片在波长 i 处的反射率。$|R_{\text{control}}(i)|$ 和 $|R_{\text{stress}}(i)|$ 的计算公式如下:

$$\left|R_{\text{control}}(i)\right| = \sqrt{\left(\sum\left(R_{\text{control}}(i) \times R_{\text{control}}(i)\right)\right)}$$
$$\left|R_{\text{stress}}(i)\right| = \sqrt{\left(\sum\left(R_{\text{stress}}(i) \times R_{\text{stress}}(i)\right)\right)} \quad (2)$$

n 的计算公式为:

$$n = \frac{\lambda_{\max} - \lambda_{\min}}{\delta} \quad (3)$$

式中,$\lambda_{\max}$ 为计算光谱角波段区间的上限,$\lambda_{\min}$ 为计算光谱角波段区间的下限,δ 为计算光谱角的波段间隔(Dennison 等,2004)。

当光谱角大于阈值 ε 时,认为光谱变异显著。阈值的计算方法如下:

$$\varepsilon_x = \arccos\left[\frac{\sum\left(R_{\text{control\_}x}(i) \times \bar{R}(i)\right)}{\left|R_{\text{control\_}x(i)}\right| \times \left|\bar{R}(i)\right|}\right]$$

$$\varepsilon = \frac{\sum_{x=1}^{q}\varepsilon_x}{q} \quad (4)$$

式中,$R_{\text{control\_}x}(i)$ 为控制组第 x 次测量的叶片反射光谱在波段 i 处的反射率,$\bar{R}(i)$ 为控制组叶片在波段 i 处的反射率均值,q 为总的测量次数。也就是说,通过计算每种植被类型控制组叶片单次测量的反射光谱与多次测量的反射光谱均值之间的差异,确定阈值。

2.3 铜污染叶片结构参数计算方法

在叶片辐射传输模型中,叶片结构是采用一个表示叶片内部空间分层情况的参数来描述。叶片结构参数是个不可测量参数,仅能通过反演光谱模拟模型得到。本文采用 PROSPECT 模型来反演叶片结构参数。PROSPECT 模型基于 Allen 的"平板模型"理论,用于模拟叶片在 400—2500 nm 的反射和透射光谱。PROSPECT 模型将叶片看成由 N 层同性层堆积起来的平板,由 $N-1$ 层空气隔开,N 为叶片结构参数。PROSPECT 模型需要 4 个输入参数:最大入射角 α、折射指数 n、结构参数 N 和总吸收系数 k(Jacquemoud 和 Baret,1990)。

在反演 N 时,研究表明,折射指数 n 无论大于或小于 1.45,反演结果都不会受影响(Feret 等,2008)。所以,首先将 n 固定为 1.45。其次,选择铜胁迫叶片 800—1200 nm 区间反射率最大的 3 个波长 $\lambda_{\max1}$、$\lambda_{\max2}$ 和 $\lambda_{\max3}$ 处的反射光谱值反演铜污染叶

片的结构参数 N_{Cu}。反演时构造的误差函数如下:

$$J\left(N_{Cu},k\left(\lambda_{max1}\right),k\left(\lambda_{max2}\right),k\left(\lambda_{max3}\right)\right)=\sum_{i=1}^{3}\left(R_{mes}\left(\lambda_{maxi}\right)-R_{mod}\left(\lambda_{maxi}\right)\right)^2 \quad (5)$$

式中,N_{Cu} 为铜污染叶片的结构参数,$k(\lambda_{max1})$ 为 λ_{max1} 处的比吸收系数,$k(\lambda_{max2})$ 为 λ_{max2} 处的比吸收系数,$k(\lambda_{max3})$ 为 λ_{max3} 处的比吸收系数,$R_{mes}(\lambda_{maxi})$ 为波长 λ_{maxi} 处测量的叶片反射光谱,$R_{mod}(\lambda_{maxi})$ 为波长 λ_{maxi} 处模型模拟的叶片反射光谱。

3 数据处理与分析

3.1 铜污染叶片反射光谱

图 1 和图 2 分别为铜污染小麦、上海青叶片的反射光谱。当胁迫浓度为 1600 μg/g、3200 μg/g 和 4800 μg/g 时,上海青发芽率基本为零。因此,对于上海青叶片,只采集了 5 个胁迫浓度的叶片反射光谱信息。与健康叶片相比,铜污染叶片反射光谱差异主要表现为反射光谱的总体抬升或者降低,其中叶片高反射波段区间(800—1300 nm)变化最明显。这种差异与时期和作物种类有关,直观上并无规律。例如,苗期和抽穗期铜污染小麦叶片反射光谱均小于健康叶片的反射光谱,但是在拔节期和灌浆期并未出现这种规律。二叶一心期铜污染上海青叶片反射光谱在可见光和中红外波段区间均小于健康叶片的反射光谱,在近红外波段区间均小于健康叶片的反射光谱;六叶一心和八叶一心期铜污染上海青叶片反射光谱均小于健康叶片的反射光谱。因此,不能通过直接观察叶片光谱区分铜污染叶片与健康叶片。

3.2 铜污染叶片光谱特征分析

研究表明,土壤与植物叶片中的 Cu 元素质量分数变化趋势相同,且两者具有较强的正相关关系(迟光宇 等,2005)。即植物叶片 Cu 累积量均随土壤中 Cu 含量增加而增加(刘素红 等,2007)。图 3 所示为小麦 7 个特征波段,从图中可以看出,随着叶片中铜含量的增加,小麦 4 个时期的紫谷、蓝边、绿峰、黄边和红谷的波段位置均没有发生明显改变,最大偏移均小于 3 nm。随着叶片中铜含量的增加,小麦苗期红边波段位置从 713 nm 移动到 719 nm,发生 6 nm红移,红肩明显红移;小麦拔节期红边波段位置从 708 nm 移动到 711 nm,发生 3 nm 红移,红肩红移;小麦抽穗期红边波段位置从 714 nm 移动到 704 nm,发生 10 nm 蓝移,红肩蓝移;小麦灌浆期红边波段位置从 712 nm 移动到 707 nm,发生 5 nm 蓝移,红肩蓝移。

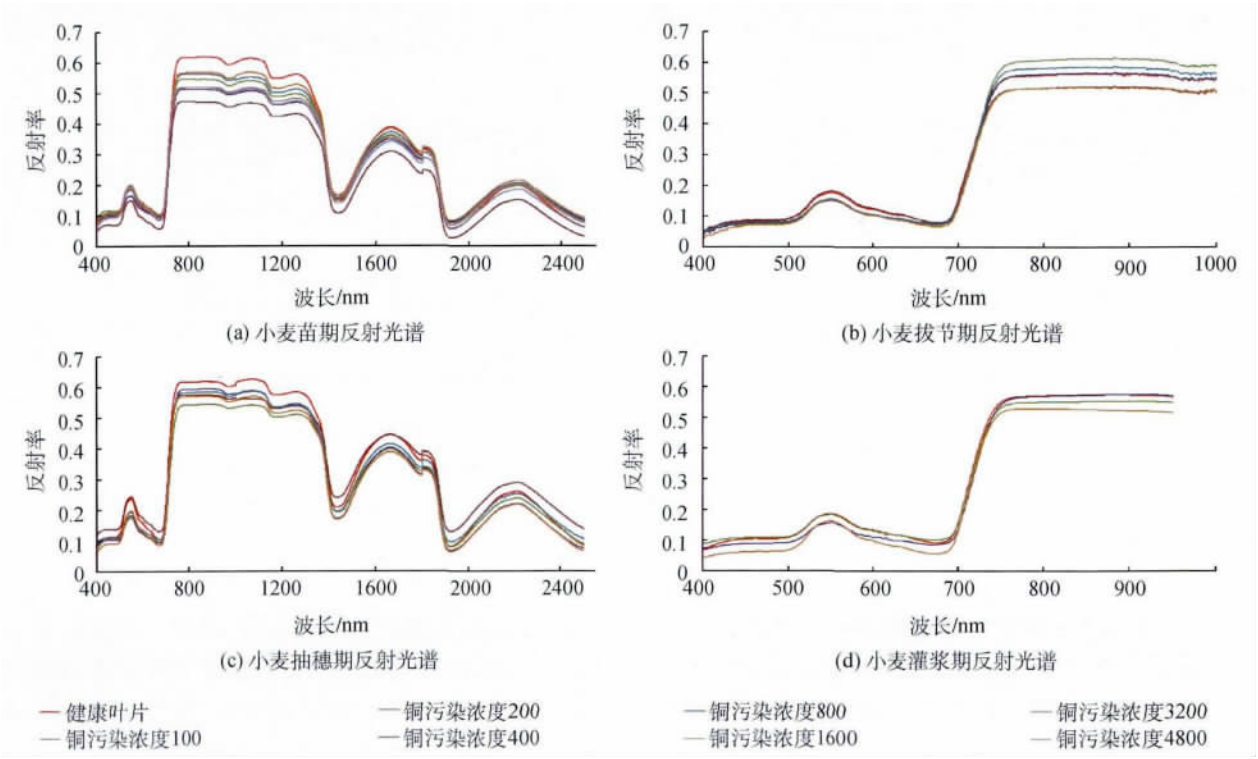

图 1 小麦叶片反射光谱

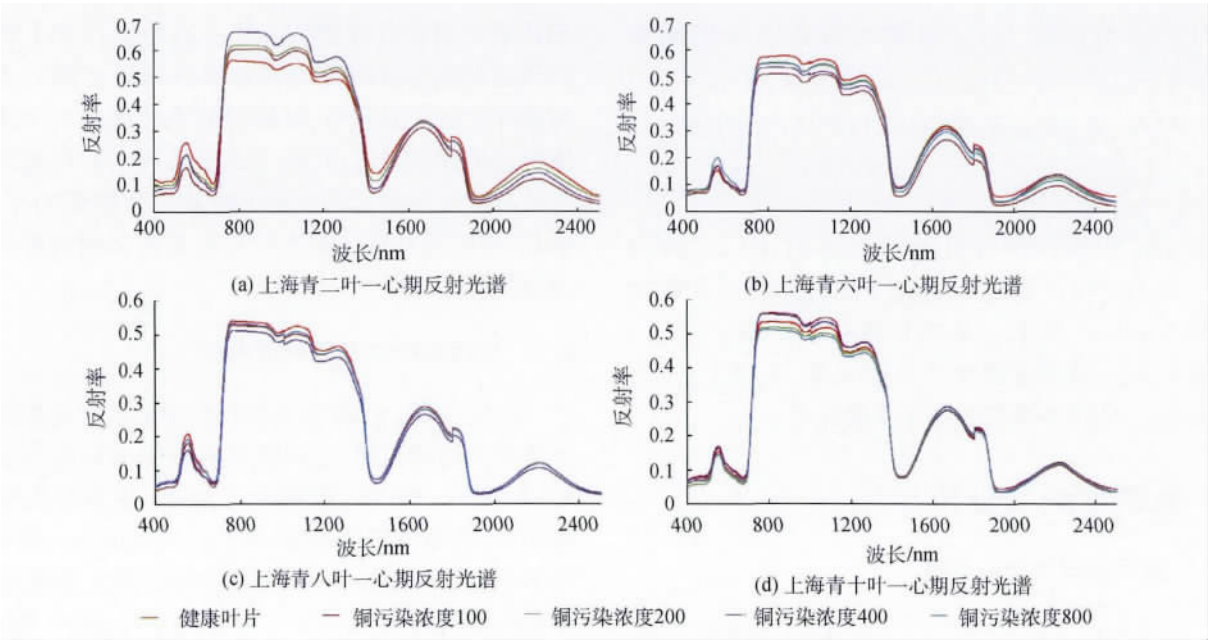

图2 上海青叶片反射光谱

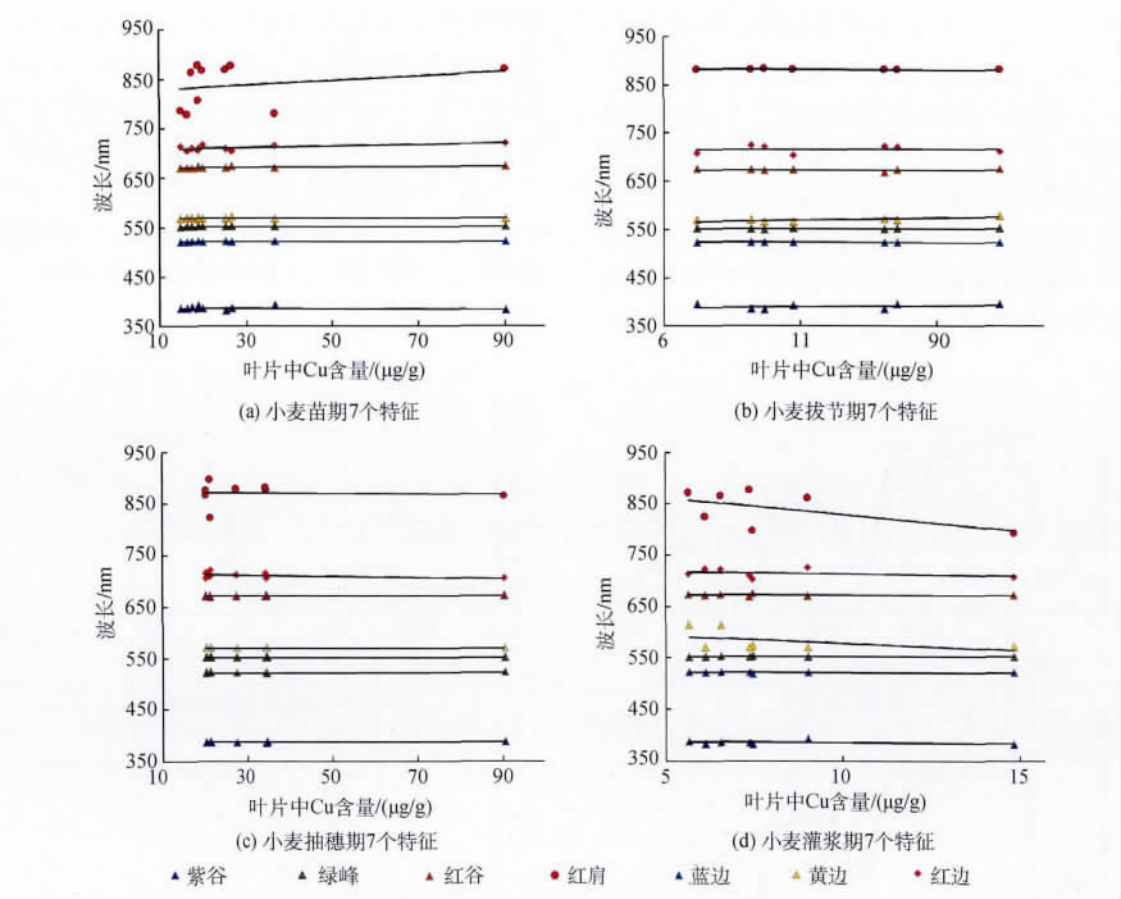

图3 小麦7个特征波段

图4所示为上海青7个特征波段。从图中可以看出,随着叶片中铜含量的增加,上海青4个时期的紫谷、蓝边、绿峰、黄边和红谷的波段位置均没有发生明显改变,最大偏移均小于3 nm,大部分在2 nm左右。随着叶片中铜含量的增加,上海青二叶一心期红边波段位置从701 nm移动到707 nm,发生6 nm蓝移,红肩明显蓝移;上海青六叶一心期红边波段位置从713 nm移动到708 nm,发生5 nm蓝移,红肩蓝移;上海青八叶一心期红边波段位置从702 nm移动到708 nm,发生6 nm红移,红肩红移;上海

青十叶一心期红边波段位置从 705 nm 移动到 711 nm,发生 6 nm 红移,红肩红移。

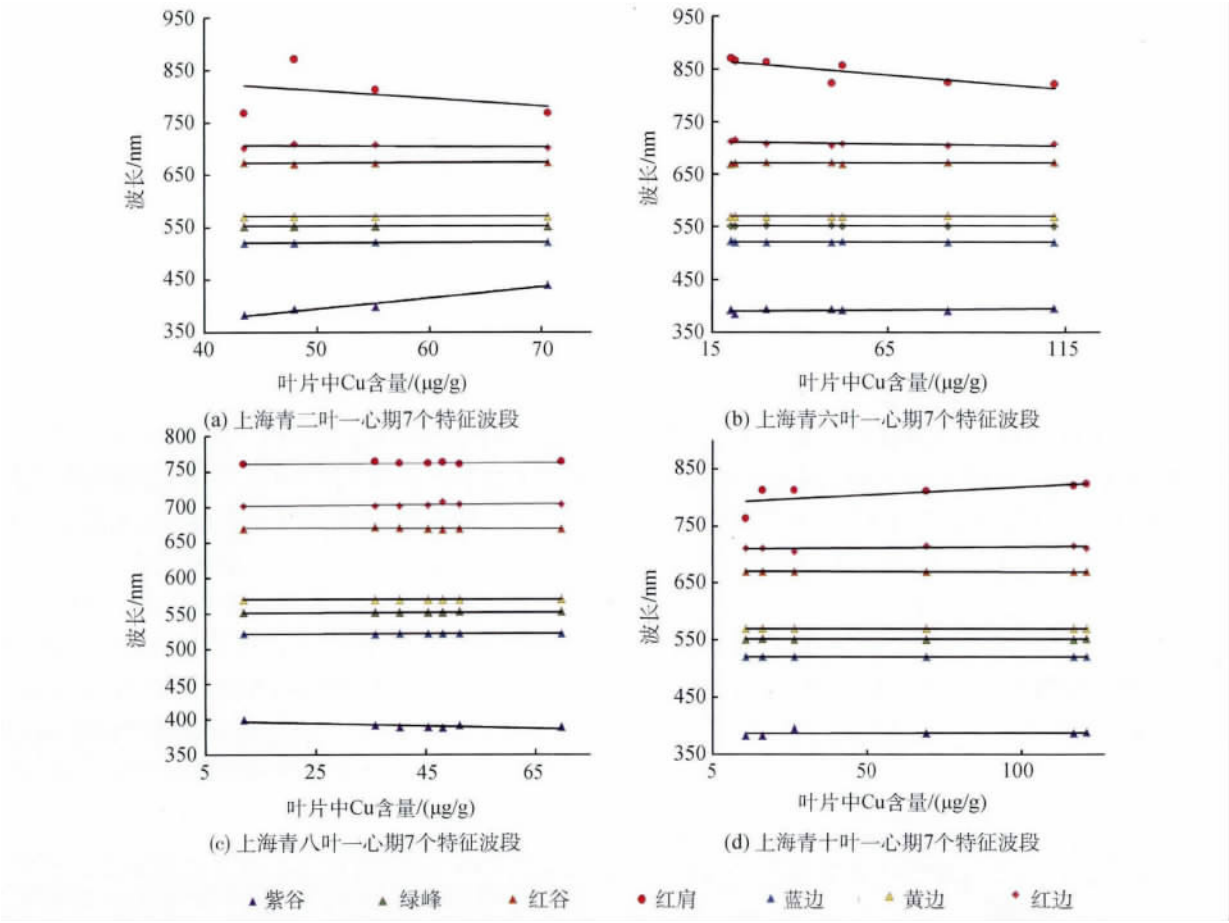

图 4 上海青 7 个特征波段

图 5 所示为重金属铜污染叶片断面扫描电镜照片。从图中可以看出,随着叶片中铜含量的增加,上表皮细胞发生分解,叶肉细胞皱缩,维管束崩解,没有了完整的维管束结构,维管束的直径变小,叶片结构更加紊乱。

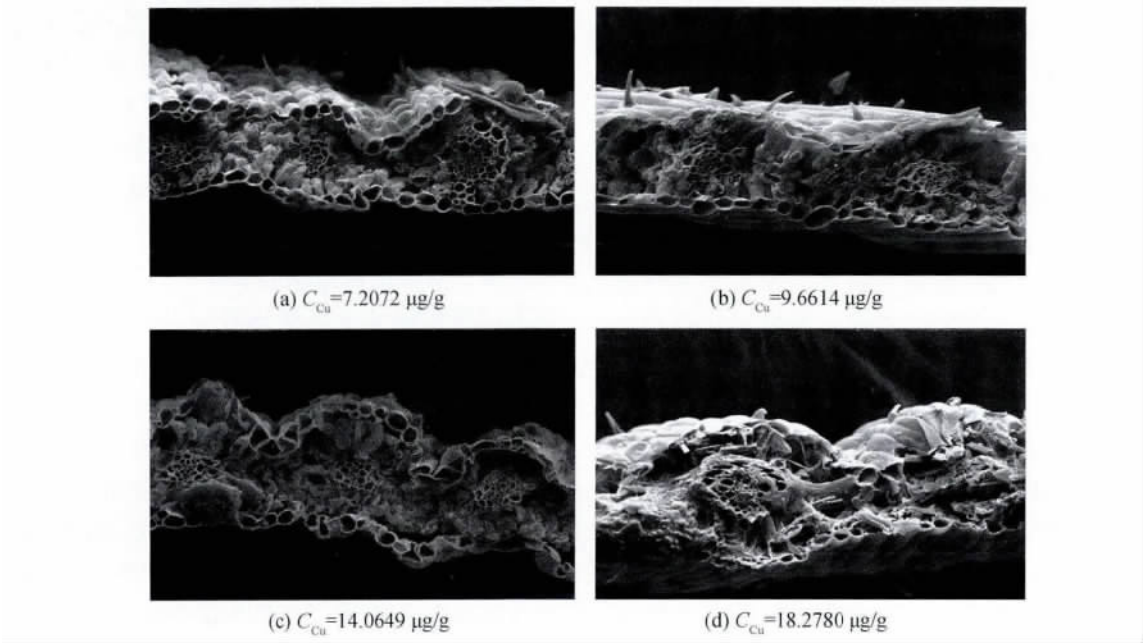

图 5 拔节期小麦横切面扫描电镜图片

图6所示为小麦和上海青红肩处反射率值与叶片结构参数 N 的关系图。在近红外谱段内,叶片的光谱特征取决于叶片内部的细胞结构(赵英时,2003)。叶片结构参数 N 描述了叶片内部结构的变化。研究表明,健康植被叶片的叶片结构参数 N 为1.5—2.5,N 越大,表明叶片内部结构越紊乱(Jacquemoud 和 Baret,1990)。从图中可以看出,铜污染叶片结构参数为3.3—4.2,明显大于健康植被叶片的结构参数 N。由此可以得出结论,铜污染使叶片内部结构更加紊乱,叶片结构参数 N 变大,这与图5所示扫描电镜照片结果是相符的。该结果很好地解释了铜污染叶片近红外谱段的光谱差异。另一方面,可以利用叶片反射光谱反演叶片结构参数 N,根据 N 值的大小来监测重金属污染:当 N 值明显高于2.5时,表明叶片内部结构变异明显,植被受到重金属污染。铜污染叶片红肩反射率值与叶片内部结构参数 N 存在明显的线性关系,红肩反射率值随着叶片内部结构参数 N 的增大而线性增加,相关系数为0.978。

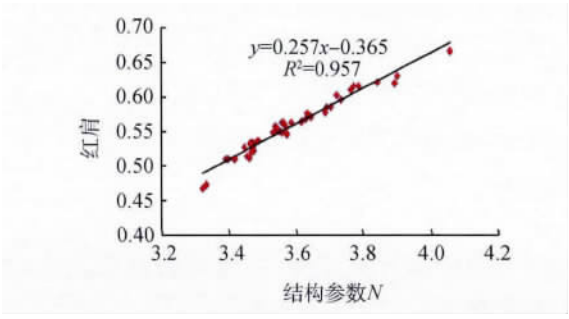

图6 铜污染叶片红肩处反射率与叶片结构参数 N 的关系图

红边是铜胁迫叶片在可见光波段范围内的主要反射特征,并且在一个生育期内呈现规律变化。研究表明,叶片红边位置主要受到受叶片内部结构和叶绿素含量的影响(梁守真 等,2010)。叶片结构参数 N 变大,红边蓝移(梁守真 等,2010)。红边红移出现的原因很复杂,但是其重要原因是因为叶黄素代替叶绿素,从而致使叶黄素含量增加叶绿素含量降低所致(Horler 等,1983)。铜胁迫小麦在苗期和拔节期营养生长旺盛,为叶绿素积累的重要时期,铜胁迫致使叶黄素含量增加、叶绿素含量减少,因此红边发生红移;抽穗期以后,小麦进入生殖生长阶段,红边位置主要受到叶片内部结构的影响,铜胁迫致使叶片内部结构更加紊乱,叶片结构参数 N 变大,因此红边发生蓝移。上海青在二叶一心期和六叶一心期的红边位置主要受到叶片内部结构的影响,铜胁迫致使叶片内部结构更加紊乱,叶片结构参数 N 变大,因此红边发生蓝移。上海青从八叶一心期开始(即播种后30—45天)进入成株期,营养生长旺盛,为叶绿素积累的重要时期,铜胁迫致使叶黄素含量增加、叶绿素含量减少,因此红边发生红移。

3.3 铜污染叶片光谱角分析

图7所示为小麦和上海青在6个波段区间的光谱角和阈值。阈值通过计算每种植被类型健康叶片单次测量的反射光谱与多次测量的反射光谱均值之间的差异确定。从图中可以看出,6个波段区间的光谱角阈值均小于0.07。当铜污染叶片光谱角大于对应阈值时,表明该叶片光谱变异显著。400—2500 nm 波段区间,90% 以上的铜污染叶片光谱变化显著;400—716 nm 表征叶绿素变化的波段区间,77% 以上的铜污染叶片光谱变化显著;717—975 nm 表征红边变化的波段区间,76% 以上的铜污染叶片光谱变化显著;976—1265 nm、1266—1770 nm 和 1771—2500 nm 3个表征水分变化的波段区间,87% 以上的铜污染叶片光谱角变化显著。

在可见光谱段内,叶片光谱主要受到叶绿素含量的影响;在近红外谱段内,叶片光谱主要取决于叶片内部细胞结构;在中红外谱段内,叶片光谱主要受到水分含量的影响(Jacquemoud 和 Baret,1990)。研究表明,植物细胞内铜离子运输跟细胞内外的铜离子浓度有关,并通过一定的受体进行运输,如果外源吸收的金属铜离子比较多,植物就会倾向于储存更多水分以尽量使离子浓度降低,减少水分蒸腾。严重的铜中毒影响叶绿素的正常生理代谢活动,造成的导致叶片变厚,叶片表面积变小,叶肉细胞间隙变少,叶片变黄甚至死亡(苟静宜,2010;王济和王世杰,2005)。这也从理论上解释了铜污染叶片的光谱差异。

基于本次实验数据分析结果表明,利用叶片光谱角检测铜污染不需要分时期、分类型讨论,只需与阈值做简单的比较,方法简便易行。一方面,光谱角对铜污染叶片 400—2500 nm 波段区间的光谱变化十分敏感。另一方面,植被对重金属铜污染十分敏感,当植物组织中的铜含量略微高于正常水平时,植被表现出明显的代谢紊乱和生长抑制(Fernandes 和 Henriques,1991)。因此,光谱角方法可以检测重金属铜污染造成的光谱变异,并基于该光谱差异监测轻度及中度(植被未发生枯死、萎黄现象)

铜污染。该方法不需要进行破坏性采样,而且对轻度铜污染十分敏感。

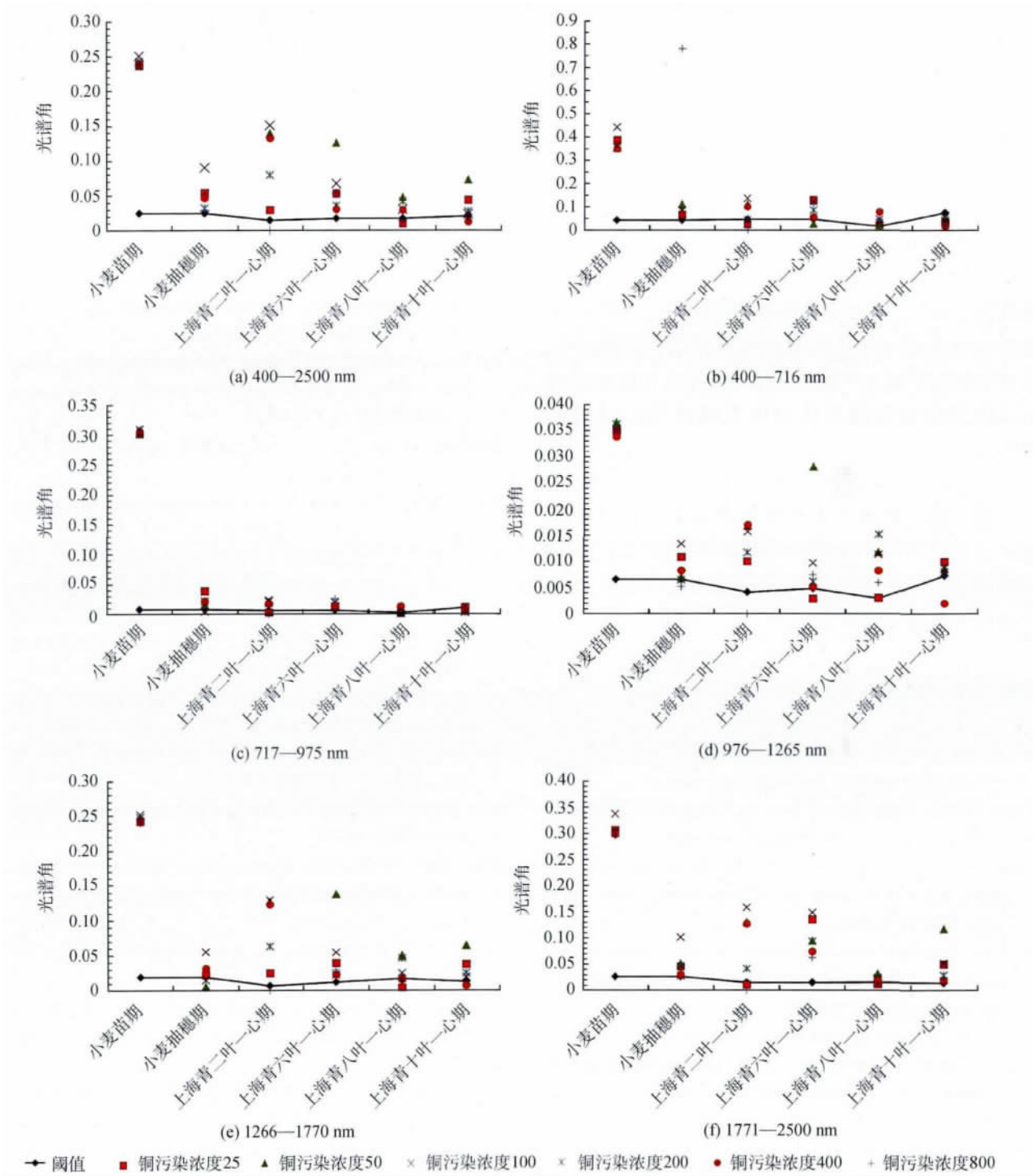

图7 6组光谱角

4 结 论

本文获取了4个不同时期、10个不同铜污染强度下的植被叶片400—2500 nm的反射光谱,并采用铜污染叶片7个特征波段和光谱角的方法探讨了铜污染叶片的光谱变化。铜污染作物栽培实验结果表明:(1)铜污染叶片反射光谱差异与作物所处时期及作物种类有关,直观上并无规律可言;(2)很难采用紫谷、蓝边、黄边、绿峰和红谷来描述铜污染叶片可见光区间的光谱差异;可以采用红边和红肩区分铜污染叶片与健康植被叶片;(3)铜污染使叶片

内部细胞结构更加紊乱,铜污染叶片结构参数 N 变大,红肩反射率值与叶片内部结构参数 N 存在线性关系,相关系数为 0.978;(4) 利用叶片光谱角检测铜污染不需要分时期、分类型讨论,只需与阈值做简单的比较,方法简便易行。而且光谱角对铜污染叶片 400—2500 nm 整个波段区间的光谱变化十分敏感。

本研究仅限于不同时期铜污染叶片光谱特征的变化以及光谱特征与叶片内部结构之间的定性关系,进一步工作需要从定量的角度分析它们之间的数量关系,并开展更为精细的室内栽培实验,从植物生理模型与叶片反射光谱模型的角度探索铜污染引起的光谱变化的内在机制,为建立重金属污染植被光谱反射物理模型提供基础理论与数据支持。

志 谢 感谢河南师范大学姬生栋教授与刘海英副教授对重金属铜胁迫植被栽培实验的支持。感谢北京师范大学王锦地教授在研究过程中提供的建设性意见与指导。

参考文献(References)

迟光宇,刘新会,刘素红,杨志峰. 2005. 大坞河流域重金属污染与五节芒光谱效应关系研究. 生态环境,14(4):549 – 554

迟光宇,刘新会,刘素红,杨志峰. 2006. Cu 污染与小麦特征光谱相关关系研究. 光谱学与光谱分析,26(7):1272 – 1276

Buschmann C, Lichtenthaler H K. 1998. Principles and characteristics of multi-colour fluorescence imaging of plants. Journal of Plant Physiology, 152(2): 297 – 314

Cho M A, Skidmore A K and Atzberger C. 2006. Towards red-edge positions less sensitive to canopy biophysical parameters using Prospect-Sailh simulated data, ISPRS

Dennison P E, Halligan K Q and Roberts D A. 2004. A comparison of error metrics and constraints for multiple endmember spectral mixture analysis and spectral angle mapper. Remote Sensing of Environment, 93(3): 359 – 367 [DOI: 10.1016/j.rse.2004.07.013]

Ebbs S D and Kochian L V. 1997. Toxicity of zinc and copper to Brassica species: implications for phytoremediation. Journal of Environmental Quality, 26(3): 776 – 781

Feret J B, Francois C, Asner G P, Gitelson A A, Martin R E, Bidel L P R, Ustin S L, le Maire G and Jacquemoud S. 2008. PROSPECT-4 and 5: Advances in the leaf optical properties model separating photosynthetic pigments. Remote Sensing of Environment, 112(6): 3030 – 3043 [DOI: 10.1016/j.rse.2008.02.012]

Fernandes J and Henriques F. 1991. Biochemical, physiological, and structural effects of excess copper in plants. The Botanical Review, 57(3): 246 – 273 [DOI: 10.1007/BF02858564]

苟静宜. 2010. 铜胁迫对紫鸭跖草生长发育的影响. 成都: 四川师范大学

Horler D, Dockray M and Barber J. 1983. The red edge of plant leaf reflectance. International Journal of Remote Sensing, 4(2): 273 – 288 [DOI: 10.1080/01431168308948546]

Horler D N H, Barber J and Barringer A R. 1980. Effects of heavy metals on the absorbance and reflectance spectra of plants

Jacquemoud S and Baret F. 1990. PROSPECT: a model of leaf optical properties spectra. Remote Sensing of Environment, 34(2): 75 – 91 [DOI: 10.1016/0034 – 4257(90)90100 – Z]

Jago R A, Cutler M E J and Curran P J. 1999. Estimating canopy chlorophyll concentration from field and airborne spectra. Remote Sensing of Environment, 68(3): 217 – 224

李娜. 2007. 重金属胁迫下矿区植物波谱异常与图像特征研究. 青岛: 山东科技大学

李庆亭,杨锋杰,张兵,张霞,周广柱. 2008. 重金属污染胁迫下盐肤木的生化效应及波谱特征. 遥感学报,12(2): 284 – 290

梁守真,施平,马万栋,邢前国,于良巨. 2010. 植被叶片光谱及红边特征与叶片生化组分关系的分析. 中国生态农业学报,18(4): 804 – 809

刘美玲,刘湘南,李婷,修丽娜. 2010. 水稻锌污染胁迫的光谱奇异性分析. 农业工程学报,26(3): 191 – 197

刘素红,刘新会,侯娟,迟光宇,崔保山. 2007. 植物光谱应用于白菜铜胁迫响应研究. 中国科学(E 辑: 技术科学),37(5): 693 – 699

刘圣伟,甘甫平,王润生. 2004. 用卫星高光谱数据提取德兴铜矿区植被污染信息. 国土资源遥感,59(1): 6 – 10,31

倪健,吴继友. 1997. 利用植物叶面反射光谱探测隐伏地下矿产. 植物学通报,14(1): 36 – 40.

瞿瑛,刘素红,李小文. 2012. 重金属 Cu 胁迫下典型农作物叶片日光诱导荧光辐射特征提取研究. 光谱学与光谱分析,32(5): 1282 – 1286

任红艳,潘剑君,张佳宝. 2005. 高光谱遥感技术的铅污染监测应用研究. 遥感信息,(3): 34 – 38

任红艳,庄大方,潘剑君,史学正,施润和,王洪杰. 2010. 重金属污染水稻的冠层反射光谱特征研究. 光谱学与光谱分析,30(2): 430 – 434

Sridhar M B B, Han F X and Diehl S V. 2007. Monitoring the effects of arsenic and chromium accumulation in Chinese brake fern (Pteris vittata), International Journal of Remote Sensing, 28(5): 1055 – 1067

谭倩,赵永超,童庆禧,郑兰芬. 2001. 植被光谱维特征提取模型. 遥感信息,1(1): 14 – 18

王济,王世杰. 2005. 土壤中重金属环境污染元素的来源及作物效应. 贵州师范大学学报(自然科学版),23(2): 113 – 120

赵江宁. 2008. 土壤铜污染对水稻生长发育的影响. 扬州: 扬州大学

赵英时. 2003. 遥感应用分析原理与方法. 北京: 科学出版社